

Subtyping of renal cortical neoplasms in fine needle aspiration biopsies using a decision tree based on genomic alterations detected by fluorescence *in situ* hybridization

Banumathy Gowrishankar, Lynnette Cahill, Alexandra E. Arndt, Hikmat Al-Ahmadie*, Oscar Lin*, Kalyani Chadalavada†, Seeta Chaganti, Gouri J. Nanjangud†, Vundavalli V. Murty‡, Raju S. K. Chaganti§, Victor E. Reuter* and Jane Houldsworth

CancerGenetics, Inc., Rutherford, NJ, Departments of *Pathology, †Molecular Cytogenetics, §Cell Biology, and Medicine, Memorial Sloan-Kettering Cancer Center, and ‡Department of Pathology and Cell Biology, Columbia University Medical Center, New York, NY, USA

Objectives

To improve the overall accuracy of diagnosis in needle biopsies of renal masses, especially small renal masses (SRMs), using fluorescence *in situ* hybridization (FISH), and to develop a renal cortical neoplasm classification decision tree based on genomic alterations detected by FISH.

Patients and Methods

Ex vivo fine needle aspiration biopsies of 122 resected renal cortical neoplasms were subjected to FISH using a series of seven-probe sets to assess gain or loss of 10 chromosomes and rearrangement of the 11q13 locus. Using specimen (nephrectomy)-histology as the 'gold standard', a genomic aberration-based decision tree was generated to classify specimens. The diagnostic potential of the decision tree was assessed by comparing the FISH-based classification and biopsy histology with specimen histology.

Results

Of the 114 biopsies diagnostic by either method, a higher diagnostic yield was achieved by FISH (92 and 96%) than histology alone (82 and 84%) in the 65 biopsies from SRMs (<4 cm) and 49 from larger masses, respectively. An optimized

decision tree was constructed based on aberrations detected in eight chromosomes, by which the maximum concordance of classification achieved by FISH was 79%, irrespective of mass size. In SRMs, the overall sensitivity of diagnosis by FISH compared with histopathology was higher for benign oncocytoma, was similar for the chromophobe renal cell carcinoma subtype, and was lower for clear-cell and papillary subtypes. The diagnostic accuracy of classification of needle biopsy specimens (from SRMs) increased from 80% obtained by histology alone to 94% when combining histology and FISH.

Conclusion

The present study suggests that a novel FISH assay developed by us has a role to play in assisting in the yield and accuracy of diagnosis of renal cortical neoplasms in needle biopsies in particular, and can help guide the clinical management of patients with SRMs that were non-diagnostic by histology.

Keywords

renal cell carcinoma, fine needle aspiration biopsies, fluorescence *in situ* hybridization, classification, algorithm, oncocytoma

Introduction

With increased use of modern imaging techniques, small renal masses (SRMs) are being identified with greater frequency, mostly in asymptomatic patients. The patient management and treatment options available for SRMs (<4 cm) include

active surveillance, thermal ablation, and partial/radical nephrectomy, the selection of which can be difficult so as to avoid overtreatment [1,2]. Importantly, more than half of all renal tumours are incidentally detected SRMs, 15–35% of which are benign and do not require surgical extirpation [3,4]. Preoperative evaluation of SRMs would help to reduce the

number of patients with benign tumours who are subjected to nephrectomy that can lead to unnecessary urological complications [5] and, in elderly patients with metastasis, this could reduce the time to initiation of selective systemic therapy, depending on tumour subtype [6]. Percutaneous image-guided needle biopsy of such masses is emerging as a valuable diagnostic tool and carries minimal risk [7,8]; however, a major challenge with needle biopsy is to obtain adequate tissue material maintaining cellular architecture for accurate histopathological diagnosis. Recent studies indicate that 10–25% of core needle biopsies are rendered non-diagnostic by histology alone [9,10]. Biopsies obtained by fine needle aspiration (FNA) have higher diagnostic rates, although with reduced accuracy [11,12]. Hence, there is a compelling need to develop ancillary assays that could assist in the accurate classification of SRMs, guiding subsequent patient management.

Renal cortical neoplasms originate in the renal cortex and comprise predominantly malignant RCC (90%) and benign oncocytoma (OC) (5%) [13]. Amongst RCCs, the clear-cell RCC (ccRCC) subtype is the most prevalent (~80–85%), with papillary (pRCC) and chromophobe RCC (chrRCC) subtypes contributing ~5–10% each. Often subtype classification can be difficult using routine morphology alone, in particular when distinguishing between OC and chrRCC, and overall ~6% of RCC remain 'unclassified' [14]. With US Food and Drug Administration approval of targeted agents such as sunitinib and temsirolimus for the treatment of metastatic ccRCC and pRCC, respectively, correct subtype classification is highly desirable. Immunohistochemical markers have variously been reported and used to assist in subtype classification, but non-specific staining can be problematic [15].

Genetic alterations have been found to be associated with each of the main renal cortical neoplasm subtypes and sometimes with prognostic value [16]. Because of its relative abundance, ccRCC has been studied most extensively, and inactivation of the *Von Hippel-Lindau* (*VHL*) gene at the 3p25 locus, mostly by deletion but also by mutation and methylation, is considered to have an aetiological role [17,18]. Gain of chromosome 5 has been linked with good prognosis in ccRCC while loss of chromosome arms 4q, 9p and 14q have been shown to be associated with poor outcome [19–22]. Gain of chromosomes 7 and 17, mostly evident as trisomies, and to some extent gain of chromosome 3, are hallmarks of pRCC [23,24]. Widespread monosomies characterize chrRCC, mostly of chromosomes 1, 2, 6, 10, 13 and 17 [25,26]. OCs often have a nearly diploid genome with frequent loss of chromosomes 1, 14 and Y [16,20,27]. Rearrangement of *CCND1* at 11q13 is also observed in OC [28,29]. Another subtype of renal cortical neoplasm exhibiting an Xp11 rearrangement occurs rarely, and mostly in a younger population [30]; therefore, subtype-associated genetic alterations offer an additional means by which the

main renal cortical neoplasm subtypes can be classified. A classification decision tree based on the presence or absence of the respective aberrations would clearly enhance implementation in a diagnostic setting.

A few studies have evaluated molecular-cytogenetic approaches such as quantitative PCR, fluorescence *in situ* hybridization (FISH) and comparative genomic hybridization, for renal tumour classification of needle biopsies [31–35]. Quantitative PCR and comparative genomic hybridization generally require a higher tumour burden compared with FISH, and are less well suited for the detection of rearrangements with relatively dispersed breakpoints [36]. FISH studies on core needle and FNA biopsies have only been performed to date assessing few aberrations on limited numbers of specimens [33–35,37]. To fully evaluate the diagnostic potential of FISH as an ancillary assay to assist in classification of needle biopsies, a large series of *ex vivo* FNA biopsies of resected renal masses were submitted to FISH, with a comprehensive series of probe sets, to detect gain, loss, and rearrangement-type aberrations of 11 chromosomes. Using the resected specimen histopathology as the 'gold standard', a novel classification decision tree was developed for molecular subtyping of renal cortical neoplasms, based on the observed genomic alterations in eight chromosomes.

Patients and Methods

Specimens

Ex vivo FNA and core needle biopsies were obtained from 132 resected renal masses from patients undergoing radical or partial nephrectomy as part of their routine care at the Memorial Sloan-Kettering Cancer Center, as previously described [11,38]. Of the 132 masses, 10 were non-renal cortical neoplasms and hence were excluded from the study. For the remaining 122, mass size was available (Table S1). ThinPreps (Hologic, Inc., Bedford, MA, USA) (4–5) were made available for FISH for each FNA biopsy. After biopsy classification by FISH (bp-FISH), the histology of the respective needle core biopsy (bp-histology) and specimen proper (sp-histology) as assessed by routine haematoxylin and eosin staining were unblinded. The sp-histology served as the gold standard (Table S1). Touch preps of adjoining normal-appearing kidney were obtained from an additional five male and five female patients with renal cancer to serve as controls for the establishment of FISH thresholds. The sex of each patient was made available to afford accurate assessment of loss of the Y chromosome. All studies were approved by the institutional review board.

Fluorescence *in Situ* Hybridization Analysis

A custom-designed series of DNA-FISH probe sets were used, as detailed in Table 1. For each locus, bacterial artificial

chromosome clones or plasmids were selected based on the genomic location and coverage of the locus of interest (Life Technologies, Grand Island, NY, USA). Individual bacterial artificial chromosomes/plasmids displaying non-specific hybridization or chimerism were excluded from the final probe sets. The individual probes were labelled by nick translation (Abbott Molecular, Des Plaines, IL, USA) incorporating one of three fluorochromes: Red 580 dUTP, Green 496 dUTP, or Gold 525 dUTP (ENZO Life Sciences Inc., Farmingdale, NY, USA) and combined according to Table 1. The ThinPrep and touch prep slides of each specimen were fixed in Carnoy's fixative (3:1, methanol: acetic acid) according to standard procedures and submitted to the series of hybridizations using an optimized protocol. Briefly, slides were pretreated with 0.1% pepsin (Sigma-Aldrich Corp., St. Louis, MO, USA) at 37°C for 30 min and then 50% glycerol/0.1X standard saline citrate (0.1X SSC) at 90 °C for 3 min. The slides were denatured in 70% formamide (Amresco LLC, Solon, OH, USA)/2X SSC for 2 min at 70°C followed by dehydration in 70 and 100% ice-cold ethanol for 4 min each and air-dried. The DNA-FISH probes were denatured at 70°C for 8 min, applied to the slides, and hybridized at 37°C overnight. Post-hybridization washes were done in 0.1% Tween-20/2X SSC at 45°C for 5 min. Slides were then counterstained with 4',6-diamidino-2-phenylindole in Vectashield anti-fade medium (Vector Laboratories, Burlingame, CA, USA) and signals visualized on a Zeiss Axioimager M1 epifluorescence microscope using fluorescence filter cubes (Chroma Technology, Bellows Falls, VT, USA). Images were captured and analysed using ISIS software (MetaSystems, Waltham, MA, USA). For a few specimens with limited material, slides were re-hybridized once with a different probe set.

For the normal control touch preps, 100 nuclei were scored each by two independent readers and the threshold values, above which specimens would be positive for the respective gains, losses and rearrangements, were calculated based on Gaussian statistics [39]. To reach 99% CI, the threshold for each probe was set at mean value in control (normal kidney) tissue plus three standard deviations. For the ThinPrep specimens, a minimum of 50 nuclei were scored for each specimen and those with <50 scorable nuclei were considered not scorable. Scoring reproducibility was evaluated by comparing scores for common probes hybridized between different probe sets (chr17 and 22) where on average, gain scores differed between hybridizations by 6.8% (SD = 9.0%) and losses by 4.1% (SD = 7.2%). The signal patterns were recorded and the presence of three or more signals for a probe was considered as gain of that probe. For each probe other than those localized to chr3 (3p21, 3p25 and 3q11), the presence of fewer than two signals was considered as loss of that probe. The score for loss of 3p, 3p21 or 3p25, was the sum of nuclei containing fewer than two signals of a probe and nuclei containing a fewer number of signals of the 3p probe with respect to the 3q11 probe. For 11q13 rearrangement, nuclei were considered to be positive for rearrangement when either individual red and/or green signals were detected along with a yellow (fusion) signal(s) in the same nucleus. The respective scores obtained for all the 122 FNA biopsies are shown in Table S1. For subtype classification, major clones and scoring patterns were taken into account, with the exception of specimens with overall low scores (<20% cells with any specific aberration) where classification was based solely on tabulated scores.

Table 1 Fluorescence *in situ* hybridization probesets and constituent bacterial artificial chromosomes.

Set	Probe (aberration)	BAC clones	Locus	Signal colour
1	3p25 (loss)	CTD-2369F5, CTD-3164K3, CTD-2252H8, CTD-3094H19	3p25 (<i>VHL</i>)	Green
	3p21 (loss)	CTD-2542H13, CTD-2653O3	3p21	Red
	3q (loss)	RP11-259L20, RP11-1133P14, RP11-95J3, RP11-90K16	3q11	Gold
2	5p (gain)	RP11-5H13, RP11-193P20, CTD-2201E9, CTD-2001E22	5p13	Green
	5q (gain)	RP11-21I20, RP11-368O19	5q33	Red
3	Chr3 (gain)	RP11-641D5, RP11-659A23, RP11-828P13, RP11-816J6	3q26	Gold
	Chr7 (gain)	RP11-667F14, RP11-354H2	7q31	Red
	Chr17 (gain)	CTD-2019C10, RP11-94L15	17q12	Green
4	Chr2 (loss)	CTD-2513E3, RP11-384J5, CTD-3049L15, RP11-418E15	2p23	Red
	Chr10 (loss)	RP11-79A15, RP11-380G5	10q23	Green
	Chr22	RP11-71J20, CTD-2505A22	22q11	Gold
	Chr6 (loss)	RP11-528A10, RP11-583F19	6p22	Red
5	Chr17 (loss)	CTD-2019C10, RP11-94L15	17q12	Green
	Chr22	RP11-71J20, CTD-2505A22	22q11	Gold
	5'- <i>CCND1</i> (rearrangement)	RP11-1109B18, RP11-166J17, RP11-729E14	11q13	Red
7	3'- <i>CCND1</i> (rearrangement)	CTD-3190C8, CTD-2612N12, RP11-109F24	11q13	Green
	Chr1 (loss)	RP11-343F16, RP11-541J2, RP11-480N10	1q23	Red
	Chr14 (loss)	RP11-521B24, RP5-998D24, RP11-417P24	14q32	Gold
	ChrY (loss)	Chromosome Yq (1-1)*	Yq12 (Satellite III)	Green

*Plasmid. BAC, bacterial artificial chromosome; *VHL*, Von Hippel-Lindau.

Statistical Analysis

Diagnostic yield and accuracy (sensitivity) were calculated based on the 114 needle biopsy specimens (65 from renal masses <4 cm and 49 from masses ≥ 4 cm in size) for which a renal cortical subtype classification could be obtained by either histology (bp-histology) or FISH (bp-FISH). For diagnostic accuracy estimates, sp-histology served as the gold standard. The percentage concordance of bp-FISH and bp-histology were calculated according to the sp-histology excluding non-diagnostic specimens by the respective methodologies.

Results

Diagnostic Yield

Fluorescence *in situ* hybridization using a panel of seven combination probe sets (Table 1) was attempted on FNA material obtained *ex vivo* from 122 resected renal cortical neoplasm masses comprising 77 ccRCCs, 19 pRCCs, 14 chrRCCs, 11 OCs and one Xp11-translocation RCC (Table S1). The mass sizes ranged from 0.6 to 15.5 cm (median, 3.7 cm) and the masses were stratified into two clinically relevant groups: 68 of <4 cm (SRMs) and 54 of ≥ 4 cm. Initially, FISH was also performed to detect the Xp11 rearrangement, but was not considered further because of sample availability limitations and the rarity of this RCC subtype, especially in the older target population in whom less invasive procedures would be mostly considered [40,41]. Thus, the Xp11-translocation RCC was excluded from further analysis. By histology alone, 27 of the remaining 121 *ex vivo* core needle biopsy specimens were non-diagnostic (22%). By FISH alone, 14 of the matching 121 *ex vivo* FNA biopsy specimens (12%) were non-diagnostic. For both methods, the frequency of non-diagnostic specimens did not differ between SRMs and larger renal masses. There were seven specimens that were not

diagnostic by either methodology, most likely because of low cellularity, and were subsequently excluded from further analyses. Table 2 lists the gold standard histology classifications of resected specimens (sp-histology) of the final 114 evaluable specimens and the respective diagnostic yield for each renal cortical neoplasm subtype obtained by histology and FISH. In SRMs (<4 cm), the FISH-based assay exhibited a higher diagnostic yield (92%) than did histology alone (82%) for *ex vivo* needle biopsies. A similar trend for increased diagnostic yield by FISH was also observed for larger renal masses (≥ 4 cm; Table 2). Importantly, FISH significantly increased the diagnostic yield over histology (89 vs 44% in SRMs) of OC which are ideal candidates for preoperative biopsy evaluation.

Development of a FISH-based Decision Tree for Renal Cortical Neoplasm Subtyping

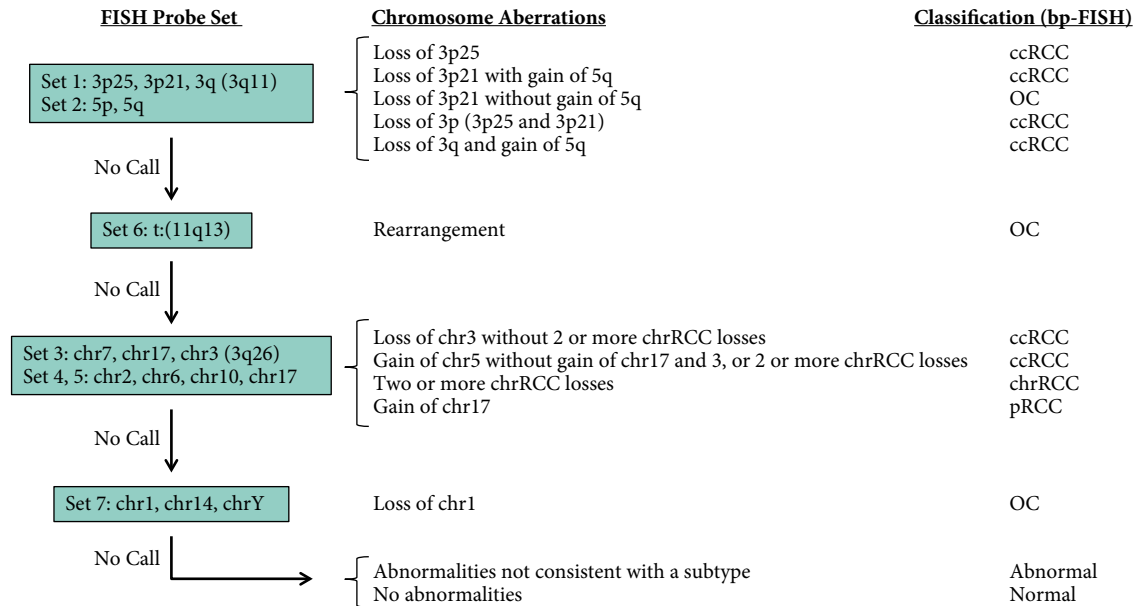
Based on the presence/absence of each FISH-detected genomic aberration (Table 1), FNA biopsies were initially assigned a renal cortical neoplasm subtype according to a preliminary decision tree considering gains and losses of 10 chromosomes and one chromosomal rearrangement based on published cytogenetic studies [16,20,23,27,37,42,43]. After unblinding of the respective sp-histology, the tree was further refined to improve the accuracy of FISH-based classification as shown in Fig. 1. The refined tree classified biopsies on the basis of gains/losses in seven chromosomes and one chromosomal rearrangement. A final subtype (bp-FISH) was then assigned to each specimen according to this tree, including classification of specimens as 'abnormal' if aberrations were present but did not result in an RCC subtype classification according to the tree and as 'normal' if no aberrations were detected. Two independent hybridizations (probe sets 1 and 2; Table 1) were required for the first

Table 2 Diagnostic yield of needle biopsy specimens by histology and fluorescence *in situ* hybridization.

sp-histology	Evaluable biopsy specimens, n (%)	Diagnostic yield	
		bp-histology, n (%)	bp-FISH, n (%)
<4 cm masses (SRMs)			
ccRCC	37	32	36
pRCC	12	11	10
chrRCC	7	6	6
OC	9	4	8
Total	65	53 (82)	60 (92)
≥ 4 cm masses			
ccRCC	35	27	35
pRCC	6	6	6
chrRCC	6	6	4
OC	2	2	2
Total	49	41 (84)	47 (96)

bp-FISH, biopsy classification by fluorescence in situ hybridization; bp-histology, needle core biopsy histology; ccRCC, clear-cell RCC; pRCC, papillary RCC; chrRCC, chromophobe RCC; OC, oncocytoma.

Fig. 1 Classification decision tree for fluorescence *in situ* hybridization (FISH)-based subtyping of renal cortical neoplasms. Specimens were assigned a renal tumour subtype based on the presence or absence of chromosomal aberrations (gain/loss/rearrangements) detected using the respective FISH probe sets according to the tree. At each decision point, if no classification could be assigned (No Call), then the results of the next hybridization(s) were considered. bp-FISH, biopsy classification by FISH.



decision point in the tree wherein most ccRCCs were classified and, as expected, included loss of the *VHL* locus characteristic of ccRCC [20]. Representative FISH images for specimen K-126 (sp-histology: ccRCC) which exhibited loss of 3p (3p25 and 3p21) are shown in Fig. 2A, which, according to the tree, was consistent with classification as ccRCC. When a specimen could not be classified based on these aberrations, then presence/absence calls were required from probe set 6 to detect rearrangement of the *CCND1* locus at 11q13, observed in OC. Such was the case for specimen K-38 (Fig. 2B) which was correctly classified as OC. The results of hybridization of probe sets 3–5 completed classification of all malignant RCC, including pRCC exemplified by specimen K-13 (sp-histology: pRCC) which showed gain of chr17 (probe set 3), typical of this subtype (Fig. 2C). Additional aberrations were observed in pRCCs, such as gain of chr7 in specimen K-13 (Fig. 2C), but because of their presence in multiple subtypes, inclusion in the tree resulted in reduced classification accuracy. Loss of chromosomes is often observed in chrRCC, in particular chr2, 6, 10 and 17 as assessed in probe sets 4 and 5, as evidenced in chrRCC specimen K-94 (Fig. 2D,E). A final hybridization (probe set 7) was required to classify remaining OC specimens. Specimen K-53 (female) was representative of OC specimens classified in this manner (Fig. 2F) showing loss of chr1. Loss of chrY and 14 were not included in the classification of OC, because of the frequent detection of aberrations involving these chromosomes in other subtypes.

Concordance of bp-FISH and bp-Histology with sp-Histology

Of the 107 renal cortical neoplasm biopsies for which a FISH-based classification was obtained (bp-FISH), the optimum concordance achieved using the refined tree was 79% (84/107, Table 3). Nine of the misclassifications were in larger masses (19%), occurring at a similar frequency to that obtained for SRMs (23%). Of the 23 misclassified specimens, 15 were frank misclassifications. Another eight specimens of those misclassified (spread evenly across SRMs and larger masses) exhibited either no aberrations or low-level clonal aberrations (<20% of cells) including aberrations not specifically scored for subtyping. This could reflect low tumour burden in these biopsies. Indeed, two of these were non-diagnostic and another 'unclassified' by routine pathology of the needle biopsy. Among the correctly classified specimens, there were seven specimens with similar low levels of clonal aberrations, of which three were non-diagnostic by histology. For such borderline specimens with <20% clonal aberrations, more accurate classification could in general be achieved by scoring additional cells to increase the confidence in the presence/absence calls of each abnormality. The bp-histology showed 97% (91/94) concordance with sp-histology for the 94 renal cortical neoplastic diagnostic specimens, with one of the three misclassifications occurring in SRMs.

Table 3 also lists the concordance of classification of diagnostic biopsies by histology alone and by FISH alone for each of the four renal cortical neoplasm subtypes. It is evident

Fig. 2 Representative fluorescence *in situ* hybridization (FISH) images of *ex vivo* renal mass FNA biopsies showing major clonal signal patterns. **(A)** Nuclei from specimen K-126 exhibiting 3p loss (3p21-red [R] and 3p25-green [G]) with respect to 3q11 (3q11-gold [Go]), consistent with clear-cell RCC subtype. **(B)** Specimen K-38 nuclei showing 11q13 rearrangement with separated 5'-*CCND1*(red) and 3'-*CCND1*(green) signals and one intact normal fusion signal (yellow [F]). **(C)** Specimen K-13 (papillary RCC) displaying gain of chr7 (red) and 17 (green), with normal copy number of 3q26 (gold). Specimen K-94 showing loss of chr2 (red) and 10 (green) in **(D)** and loss of chr6 in **(E)**, classified as chromophobe RCC. **(F)** OC specimen K-53 (female) showing monosomy of chr1 (red). BA, breakapart FISH probe.

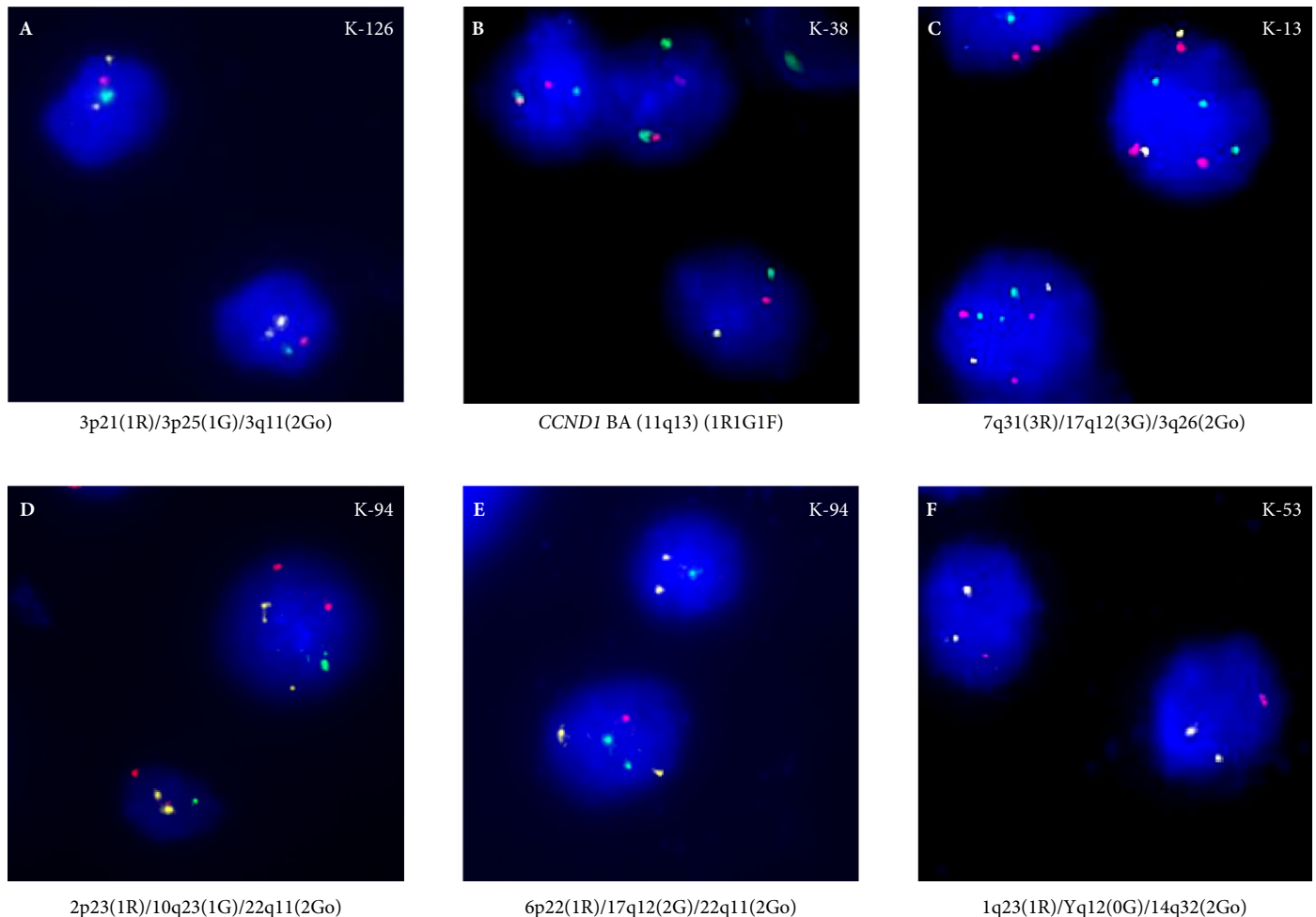


Table 3 Concordance of biopsy classification by needle core biopsy histology and by fluorescence *in situ* hybridization with histology of resected specimens.

sp-Histology	Histology concordance		FISH concordance	
	bp-Histology	%	bp-FISH	%
ccRCC	59/59	100	60/71	85
pRCC	16/17	94	11/16	69
chrRCC	11/12	92	6/10	60
OC	5/6	83	7/10	70
Total	91/94	97	84/107	79

FISH, fluorescence *in situ* hybridization; bp-FISH, biopsy classification by FISH; bp-histology, needle core biopsy histology; sp-histology, specimen histology; ccRCC, clear-cell RCC; pRCC, papillary RCC; chrRCC, chromophobe RCC; OC, oncocytoma.

that histology outperformed FISH in each of the four subtypes. The reduced concordance of ccRCC classification by FISH was mostly the result of misclassification as pRCC (seven of 11 specimens). Interestingly, for five of these specimens, large clonal populations of cells showed gain of chr3, 5, and 17 (probe sets 2 and 3) but none showed loss of 3p25 (*VHL*) or 3p, scored relative to 3q11 in probe set 1. Examination of the scoring patterns of probe set 1 for these five specimens revealed no gain of 3p25, 3p21, or 3q11 loci, distinct from that found in probe set 3 for the 3q26 locus. This is exemplified by specimen K-105 in Fig. 3. Thus, relative to 3q26, these five specimens exhibited loss of 3p and 3q11, resulting in the correct classification of the specimens as ccRCC. Such segmental duplication of 3q has previously been

Fig. 3 Segmental aneuploidy of chr3 in clear-cell RCC as revealed by fluorescence *in situ* hybridization (FISH). Representative FISH images of probe sets 1 (A) and 3 (B) are shown for the specimen K-105. Major clonal signal patterns are listed below each image.

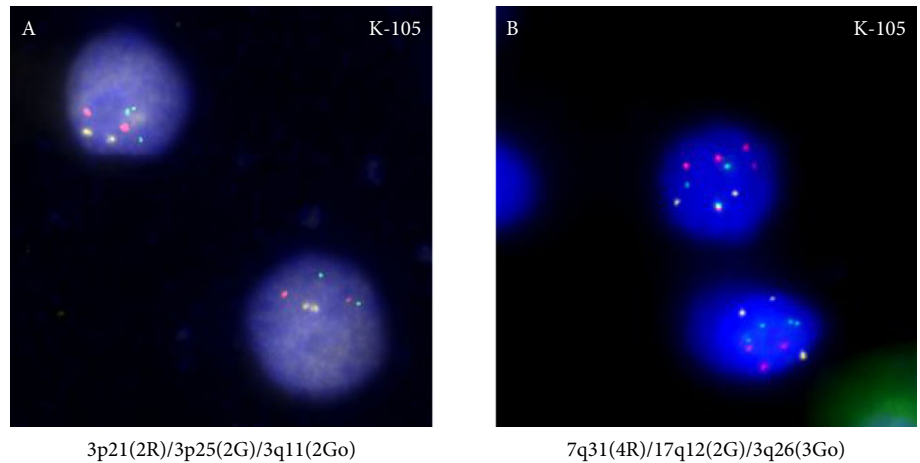


Table 4 Combined diagnostic accuracy of biopsy classification by histology and by fluorescence *in situ* hybridization for renal tumour subtyping in needle biopsies.

sp-histology	Evaluable biopsy specimens (n)	Diagnostic accuracy		
		bp-histology, n (%)	bp-FISH, n (%)	bp-histology+bp-FISH, n (%)
<4 cm masses (SRMs)				
ccRCC	37	32	28	36
pRCC	12	11	7	12
chrRCC	7	5	5	6
OC	9	4	6	7
Total	65	52 (80)	46 (71)	61 (94)
≥4 cm masses				
ccRCC	35	27	32	35
pRCC	6	5	4	5
chrRCC	6	6	1	6
OC	2	1	1	2
Total	49	39 (80)	38 (78)	48 (98)
Combined total	114	91 (80)	84 (74)	109 (96)

FISH, fluorescence *in situ* hybridization; bp-FISH, biopsy classification by FISH; bp-histology, needle core biopsy histology; sp-histology, specimen histology; ccRCC, clear-cell RCC; pRCC, papillary RCC; chrRCC, chromophobe RCC; OC, oncocytoma.

reported in ccRCC [44]. For the remaining two ccRCCs misclassified as pRCC, gains of 3p25, 3p21, and 3q11 were found, and it is possible in these cases that *VHL* was inactivated by other mechanisms such as mutation or methylation rather than deletion [17,18]. Three of the five misclassified pRCCs, exhibited alterations consistent with ccRCC (one with <20% clonal abnormalities) but no common reason for misclassification was evident. Three of the four misclassified chrRCCs, were called ccRCC, of which one had low tumour burden. Another was from a patient with Birt-Hogg-Dube syndrome, wherein mutations in *FLCN* predispose carriers to chromophobe/oncocytic/hybrid renal tumours [45]. It is unclear if the genomic alterations associated within the Birt-Hogg-Dube subtype of chrRCC are similar to those observed in sporadic chrRCC, perhaps explaining the misclassification by FISH. One other chrRCC was also misclassified by histology. For OC,

three were misclassified by FISH, one as a result of low tumour burden.

Diagnostic Accuracy

The diagnostic accuracy of classification was calculated for the 114 evaluable renal cortical neoplasm biopsies by FISH (bp-FISH) and histology (bp-histology) inclusive of non-diagnostic specimens relative to the resected specimen histology (sp-histology) and stratified according to mass size (Table 4). Across all the evaluable specimens obtained from SRMs, histology and FISH assays yielded similar overall diagnostic accuracies when considered individually: 79% by histology vs 71% by FISH; however, on combining the results obtained by FISH with those obtained by histology alone, the overall diagnostic accuracy of classification of needle biopsy

specimens from SRMs increased from 80%, obtained by histology alone, to 94% (Table 4). A similar increase in combined diagnostic accuracy was also evident for biopsies from renal masses ≥ 4 cm. In SRMs, the overall diagnostic accuracy by FISH was improved for OC, was similar for chrRCC, and lower for ccRCC and pRCC subtypes with respect to histopathology. Across all masses, the sensitivity of diagnosis of ccRCC was similar for histology and FISH. Histology was more sensitive in the classification of pRCC and chrRCC than FISH, but the reverse was evident for OC. Except for ccRCC, FISH yielded similar overall specificities to those for histology (Table S2).

Discussion

Use of image-guided needle biopsies has increased in recent years for diagnostic evaluation of a variety of cancers to assist in clinical management, including diagnosis of SRMs to guide appropriate intervention. Risk stratification of SRMs has benefited from core and FNA biopsies obtained by minimally invasive procedures for morphological examination, when compared with imaging alone [1,6]; however, working with such biopsy material is challenging, largely because of insufficient sample cellularity and damaged tissue integrity. Additionally, in the case of FNA biopsies, cytology, while useful to distinguish benign from malignant lesions, has reduced the ability to differentiate non-ccRCC subtypes [11]. Depending on the clinical need, molecular-cytogenetic methodologies offer an additional diagnostic tool to assist in specimen characterization. In the present study, the potential of FISH to serve as an adjunctive assay in the diagnostic classification of needle biopsies of renal cortical neoplasms was explored. A large panel of *ex vivo* FNA biopsies from both SRMs and larger renal masses was subjected to a series of seven FISH probeset hybridizations designed to assess genomic abnormalities commonly found in each of the four subtypes of renal cortical neoplasms. The FISH assay was found to have the potential for an overall higher diagnostic yield than morphology alone in the case of SRMs as well as larger renal masses (≥ 4 cm). A novel classification decision tree was built based on the presence/absence of genomic abnormalities observed in eight chromosomes, and according to the tree, the overall sensitivity of classification of FISH vs morphology were similar for ccRCC, lower for chrRCC and pRCC, but higher for OC. Notably, inclusion of the FISH-based assay and algorithm for renal cortical neoplasm subtyping increased the overall diagnostic accuracy by 14% from morphology alone for SRMs. In addition, application of this assay to those RCC specimens that remain 'unclassified' by routine pathology would clearly assist in RCC subtyping for therapy guidance. Before the present study, only few others had evaluated FISH in the classification of renal cortical neoplasms in needle biopsies but with much reduced sample numbers and assessing fewer genomic aberrations [33,35].

Multiple genomic abnormalities have been reported to be associated with the different renal cortical neoplasm subtypes [33,37,42,46]. The panel of probes in the present study were designed to detect gains/losses of 10 chromosomes (chromosomes 1, 2, 3 [four loci], 5 [two loci], 6, 7, 10, 14, 17, and Y) and rearrangement of the 11q13 locus. The final algorithm that was built required fewer probes comprising chromosomes 1, 2, 3 (three loci), 5q, 6, 10, and 17 and rearrangement at 11q13. This is clearly an important consideration for specimens such as needle biopsies with limited tissue availability. Feasibly, as few as four hybridizations (three probes per hybridization) would be sufficient to assess the genomic aberrations required for classification. A sequential series of the four hybridizations could also potentially be invoked where, if biopsies exhibit alterations in chromosomes 3 and 5 according to the tree that permit classification at the first decision point (Fig. 1), then no further hybridizations would be required. In general, the chromosomal abnormalities in the final algorithm comprised those reported in the literature for specific subtypes. Interestingly, however, deletion at the 3p21 locus was found to be associated with OC and was observed in two of the 10 OC specimens as a classifying abnormality when observed without the gain of 5q that is commonly detected in ccRCC. Loss of heterozygosity at 3p21 in OC has been reported in one previous study, although the target gene and exact role in this benign neoplasm is unclear [47]. Validation of this novel genomic marker to assist in classification of OC is required in a larger sample set. In ccRCC, mutational inactivation of the *PBRM1* gene mapped to 3p21 has been implicated in tumorigenesis and also recently suggested to be associated with longer overall survival [48].

Despite optimization of the decision tree, FISH alone was not found to be as accurate in classification of needle biopsies as morphology. This was because of low clonal tumour populations, inability to correctly identify miscellaneous renal neoplasms (other than RCC and OC), and frank misclassifications. The first problem could be addressed by increasing the number of nuclei scored in biopsies with low levels of detected abnormalities. Notably, in the present study, the numbers of nuclei scored were similar to other studies [33,35]. The second is an inherent pitfall of the assay attributable to the assessment only of chromosomal anomalies frequent in renal cortical neoplasms and supports the role of FISH as an ancillary test to morphology to assist in classification rather than a stand-alone test using the current panel of probes. The last reason for misclassification could be accounted for by segmental duplication of chr3 (could be avoided by using a 3q26 probe for scoring 3p loss), alterations in target genes either below the resolution of detection by FISH, at other discriminatory loci not in the current panel, or by other genetic or epigenetic mechanisms of gene activation/inactivation. This is exemplified in ccRCC, where

VHL can also undergo inactivation by mutation and/or methylation [17,18]. Recent studies have clearly underscored the role of such mechanisms, not only in renal cancer aetiology but also in metastasis [49].

Image-guided needle biopsies of renal masses are currently recommended for poor surgical candidates and elderly patients with comorbidities [50]. Accurate diagnosis of the limited available tissue is highly desirable, especially in the context of SRMs, wherein about one third of masses were diagnosed to be benign. About 20% of core needle biopsies in the present study were non-diagnostic by histopathology alone, reducing the potential for this procedure to assist in patient management. A supporting role for FISH in renal tumour classification of needle biopsies was demonstrated in this *ex vivo* study to enhance the overall diagnostic accuracy by 16% compared with histopathology alone. The greatest diagnostic potential for the FISH assay was evident for SRMs that were non-diagnostic by core biopsy histology. The FISH assay also exhibited the potential to diagnose 'unclassified-RCC' specimens, exemplified by specimen K-67 that was correctly classified by FISH as OC. In addition, FISH was found to be particularly superior for the detection of OC, a benign subtype for which active surveillance is recommended, avoiding overtreatment, an important consideration in an older frail population. The diagnostic accuracy of FISH testing of core needle biopsies instead of FNA biopsies requires further evaluation; however, given the overall limited tissue availability of needle biopsy specimens, it is feasible that other DNA-based assays, including a comparative genomic hybridization to permit evaluation of genomic gain/loss at additional loci not targeted by FISH, targeted massively parallel sequencing for select genes, and methylation, or a combination thereof with FISH could be implemented to improve the overall accuracy of diagnosis. The costs of performing and the reporting times of these higher complexity assays become important considerations in routine renal mass patient care and management. Comparison of the diagnostic accuracy of these methodologies in a clinical setting is warranted.

Acknowledgements

We thank Subhadra Nandula for useful discussions and critical reading of the manuscript. The work was funded in part by the NIH (CA134103; J.H.) and by the College of American Pathologist Foundation Scholars Program (H.A.).

Conflict of Interest

H.A.-A. reports grants from the College of American Pathologists. A.E.A., L.C., B.G., S.C., and J.H. are employees of Cancer Genetics, Inc. and hold stock options. R.S.K.C. reports personal fees and other from Cancer Genetics, Inc. and outside the submitted work. In addition, R.S.K.C. and J.H. have

a patent pending. J.H. also reports grants from NIH during the conduct of the study. K.C., O.L., V.V.M., G.J.N. and V.E.R. have nothing to disclose.

References

- 1 Alasker A, Williams SK, Ghavamian R. Small renal mass: to treat or not to treat. *Curr Urol Rep* 2013; 14: 13–8
- 2 Volpe A, Cadeddu JA, Cestari A et al. Contemporary management of small renal masses. *Eur Urol* 2011; 60: 501–15
- 3 Remzi M, Marberger M. Renal tumor biopsies for evaluation of small renal tumors: why, in whom, and how? *Eur Urol* 2009; 55: 359–67
- 4 Wang R, Wood DP Jr. Evolving role of renal biopsy in small renal masses. *Urol Oncol* 2009; 27: 332–4
- 5 Thomas AA, Campbell SC. Small renal masses: toward more rational treatment. *Cleve Clin J Med* 2011; 78: 539–47
- 6 Volpe A, Finelli A, Gill IS et al. Rationale for percutaneous biopsy and histologic characterisation of renal tumours. *Eur Urol* 2012; 62: 491–504
- 7 Samplaski MK, Zhou M, Lane BR, Herts B, Campbell SC. Renal mass sampling: an enlightened perspective. *Int J Urol* 2011; 18: 5–19
- 8 Laguna MP, Kummerlin I, Rioja J, De La Rosette JJ. Biopsy of a renal mass: where are we now? *Curr Opin Urol* 2009; 19: 447–53
- 9 Leveridge MJ, Finelli A, Kachura JR et al. Outcomes of small renal mass needle core biopsy, nondiagnostic percutaneous biopsy, and the role of repeat biopsy. *Eur Urol* 2011; 60: 578–84
- 10 Shannon BA, Cohen RJ, De Bruto H, Davies RJ. The value of preoperative needle core biopsy for diagnosing benign lesions among small, incidentally detected renal masses. *J Urol* 2008; 180: 1257–61
- 11 Adeniran AJ, Al-Ahmadie H, Iyengar P, Reuter VE, Lin O. Fine needle aspiration of Renal cortical lesions in adults. *Diagn Cytopathol* 2010; 38: 710–5
- 12 Barwari K, Kummerlin IP, Ten Kate FJ et al. What is the added value of combined core biopsy and fine needle aspiration in the diagnostic process of renal tumours? *World J Urol* 2013; 31: 823–7
- 13 Kovacs G, Akhtar M, Beckwith BJ et al. The Heidelberg classification of renal cell tumours. *J Pathol* 1997; 183: 131–3
- 14 Lopez-Beltran A, Carrasco JC, Cheng L, Scarpelli M, Kirkali Z, Montironi R. 2009 update on the classification of renal epithelial tumors in adults. *Int J Urol* 2009; 16: 432–43
- 15 Shen SS, Truong LD, Scarpelli M, Lopez-Beltran A. Role of immunohistochemistry in diagnosing renal neoplasms: when is it really useful? *Arch Pathol Lab Med* 2012; 136: 410–7
- 16 Hagenkord JM, Gatalica Z, Jonasch E, Monzon FA. Clinical genomics of renal epithelial tumors. *Cancer Genet* 2011; 204: 285–97
- 17 Herman JG, Latif F, Wang Y et al. Silencing of the *VHL* tumor-suppressor gene by DNA methylation in renal carcinoma. *Proc Natl Acad Sci USA* 1994; 91: 9700–4
- 18 Kim WY, Kaelin WG. Role of *VHL* gene mutation in human cancer. *J Clin Oncol* 2004; 22: 4991–5004
- 19 Chen M, Ye Y, Yang H et al. Genome-wide profiling of chromosomal alterations in renal cell carcinoma using high-density single nucleotide polymorphism arrays. *Int J Cancer* 2009; 125: 2342–8
- 20 Klatt T, Rao PN, De Martino M et al. Cytogenetic profile predicts prognosis of patients with clear cell renal cell carcinoma. *J Clin Oncol* 2009; 27: 746–53
- 21 Lopez-Lago MA, Thodima VJ, Guttapalli A et al. Genomic deregulation during metastasis of renal cell carcinoma implements a myofibroblast-like program of gene expression. *Cancer Res* 2010; 70: 9682–92
- 22 Gunawan B, Huber W, Holtrup M et al. Prognostic impacts of cytogenetic findings in clear cell renal cell carcinoma: gain of 5Q31-QTER predicts a distinct clinical phenotype with favorable prognosis. *Cancer Res* 2001; 61: 7731–8

- 23 Klatte T, Pantuck AJ, Said JW et al. Cytogenetic and molecular tumor profiling for type 1 and type 2 papillary renal cell carcinoma. *Clin Cancer Res* 2009; 15: 1162–9
- 24 Szponar A, Zubakov D, Pawlak J, Jauch A, Kovacs G. Three genetic developmental stages of papillary renal cell tumors: duplication of chromosome 1Q marks fatal progression. *Int J Cancer* 2009; 124: 2071–6
- 25 Yusenko MV, Kuiper RP, Boethe T, Ljungberg B, Van Kessel AG, Kovacs G. High-resolution DNA copy number and gene expression analyses distinguish chromophobe renal cell carcinomas and renal oncocytomas. *BMC Cancer* 2009; 9: 152
- 26 Speicher MR, Schoell B, Du Manoir S et al. Specific loss of chromosomes 1, 2, 6, 10, 13, 17, and 21 in chromophobe renal cell carcinomas revealed by comparative genomic hybridization. *Am J Pathol* 1994; 145: 356–64
- 27 Reutzel D, Mende M, Naumann S et al. Genomic imbalances in 61 renal cancers from the proximal tubulus detected by comparative genomic hybridization. *Cytogenet Cell Genet* 2001; 93: 221–7
- 28 Sukov WR, Ketterling RP, Lager DJ et al. CCND1 rearrangements and cyclin d1 overexpression in renal oncocytomas: frequency, clinicopathologic features, and utility in differentiation from chromophobe renal cell carcinoma. *Hum Pathol* 2009; 40: 1296–303
- 29 Jhang JS, Narayan G, Murty VV, Mansukhani MM. Renal oncocytomas with 11q13 rearrangements: cytogenetic, molecular, and immunohistochemical analysis of cyclin d1. *Cancer Genet Cytogenet* 2004; 149: 114–9
- 30 Lopez-Beltran A, Scarpelli M, Montironi R, Kirkali Z. 2004 WHO classification of the renal tumors of the adults. *Eur Urol* 2006; 49: 798–805
- 31 Barocas DA, Rohan SM, Kao J et al. Diagnosis of renal tumors on needle biopsy specimens by histological and molecular analysis. *J Urol* 2006; 176: 1957–62
- 32 Vieira J, Henrique R, Ribeiro FR et al. Feasibility of differential diagnosis of kidney tumors by comparative genomic hybridization of fine needle aspiration biopsies. *Genes Chromosomes Cancer* 2010; 49: 935–47
- 33 Barocas DA, Mathew S, Delpizzo JJ et al. Renal cell carcinoma sub-typing by histopathology and fluorescence in situ hybridization on a needle-biopsy specimen. *BJU Int* 2007; 99: 290–5
- 34 Chyhray A, Sanjmyatav J, Gajda M et al. Multi-colour fish on preoperative renal tumour biopsies to confirm the diagnosis of uncertain renal masses. *World J Urol* 2010; 28: 269–74
- 35 Roh MH, Dal Cin P, Silverman SG, Cibas ES. The application of cytogenetics and fluorescence in situ hybridization to fine-needle aspiration in the diagnosis and subclassification of renal neoplasms. *Cancer Cytopathol* 2010; 118: 137–45
- 36 Speicher MR, Carter NP. The new cytogenetics: blurring the boundaries with molecular biology. *Nat Rev Genet* 2005; 6: 782–92
- 37 Receveur AO, Couturier J, Molinier V et al. Characterization of quantitative chromosomal abnormalities in renal cell carcinomas by interphase four-color fluorescence in situ hybridization. *Cancer Genet Cytogenet* 2005; 158: 110–8
- 38 Al-Ahmadie HA, Alden D, Fine SW et al. Role of immunohistochemistry in the evaluation of needle core biopsies in adult renal cortical tumors: an ex vivo study. *Am J Surg Pathol* 2011; 35: 949–61
- 39 Ciolino AL, Tang ME, Bryant R. Statistical treatment of fluorescence in situ hybridization validation data to generate normal reference ranges using excel functions. *J Mol Diagn* 2009; 11: 330–3
- 40 Campbell SC, Novick AC, Beldegrun A et al. Guideline for management of the clinical T1 renal mass. *J Urol* 2009; 182: 1271–9
- 41 Armah HB, Parwani AV. XP11.2 Translocation renal cell carcinoma. *Arch Pathol Lab Med* 2010; 134: 124–9
- 42 Bugert P, Gaul C, Weber K et al. Specific genetic changes of diagnostic importance in chromophobe renal cell carcinomas. *Lab Invest* 1997; 76: 203–8
- 43 Sanjmyatav J, Schubert J, Junker K. Comparative study of renal cell carcinoma by CGH, multicolor-FISH and conventional cytogenetic banding analysis. *Oncol Rep* 2005; 14: 1183–7
- 44 Brunelli M, Fiorentino M, Gobbo S et al. Many facets of chromosome 3P cytogenetic findings in clear cell renal carcinoma: the need for agreement in assessment fish analysis to avoid diagnostic errors. *Histol Histopathol* 2011; 26: 1207–13
- 45 Linehan WM, Pinto PA, Bratslavsky G et al. Hereditary kidney cancer: unique opportunity for disease-based therapy. *Cancer* 2009; 115: 2252–61
- 46 Krill-Burger JM, Lyons MA, Kelly LA et al. Renal cell neoplasms contain shared tumor type-specific copy number variations. *Am J Pathol* 2012; 180: 2427–39
- 47 El-Naggar AK, Batsakis JG, Wang G, Lee MS. PCR-based RFLP screening of the commonly deleted 3P loci in renal cortical neoplasms. *Diagn Mol Pathol* 1993; 2: 269–76
- 48 Kapur P, Pena-Llopis S, Christie A et al. Effects on survival of BAP1 and PBRM1 mutations in sporadic clear-cell renal-cell carcinoma: a retrospective analysis with independent validation. *Lancet Oncol* 2013; 14: 159–67
- 49 Vanharanta S, Shu W, Brenet F et al. Epigenetic expansion of VHL-HIF signal output drives multiorgan metastasis in renal cancer. *Nat Med* 2013; 19: 50–6
- 50 Mally AD, Gayed B, Averch T, Davies B. The current role of percutaneous biopsy of renal masses. *Can J Urol* 2012; 19: 6243–9

Correspondence: Jane Houldsworth, Cancer Genetics, Inc. 201 Route 17 North, Rutherford, NJ 07070, USA.

e-mail: jhouldsworth@cancergenetics.com

Abbreviations: SRM, small renal mass; FISH, fluorescence in situ hybridization; FNA, fine needle aspiration; OC, oncocytoma; ccRCC, clear-cell RCC; pRCC, papillary RCC; chrRCC, chromophobe RCC; *VHL*, *Von Hippel-Lindau*; bp-FISH, biopsy classification by FISH; bp-histology, needle core biopsy histology; sp-histology, specimen histology.

Supporting Information

Additional Supporting Information may be found in the online version of this article at the publisher's web-site:

Table S1 Percentage of abnormal fluorescence *in situ* hybridization (FISH) signal patterns in nuclei of 122 *ex vivo* fine needle aspiration biopsies. Also given is the size of the renal mass, resected specimen histology (sp-histology), core needle biopsy histology (bp-histology), and FISH-based biopsy classification (bp-FISH) for each specimen.

Table S2 Sensitivity (diagnostic accuracy) and specificity of each renal cortical neoplasm subtype classification by core needle biopsy histology (bp-histology) and fluorescence *in situ* hybridization (FISH)-based biopsy classification (bp-FISH) of all the renal masses (irrespective of size) used in this study.